Energy-loss spectrum of swift ions in charge-state equilibrium

Lev G. Glazov*
Physics Department, Odense University, DK-5230 Odense M, Denmark
and Institute of High Current Electronics, Akademicheski 4, Tomsk Russia
(Received 31 July 1997; revised manuscript received 3 November 1997)

The energy-loss spectrum of ions in the presence of charge exchange is analyzed theoretically for large path lengths. The evaluation is based upon steepest-descent integration of the generalized Bothe-Landau formula. General approximation formulas for the spectrum are derived without reference to particular collision cross sections, and their regions of validity are discussed. The approximations are tested against numerical curves for 32-MeV ^{3}He ions in carbon. General asymptotic expressions for the peak energy loss and half-widths of the spectrum are found. The asymptotic expression for the mean-to-peak interval is specified and analyzed. In particular, it is shown and illustrated on a model system that the sign of the difference between the peak and mean energy loss may be opposite to that in the one-state case. [S1050-2947(98)03404-0]

PACS number(s): 34.50.Bw, 34.70.+e, 52.40.Hf, 61.85.+p

I. INTRODUCTION

The problem of determining the energy-loss spectrum of charged particles penetrating a layer of material has been extensively studied for pointlike particles [1–3] under the assumption that the mean energy loss is small compared to the initial ion energy. For sufficiently fast ions, the dominant energy-loss mechanism is electronic stopping: excitation and ionization of target atoms. The spectrum may be approximated by a Gaussian [4,1] when the path length is large enough so that $\Omega \gg T_m$, where Ω^2 is the straggling and T_m the maximum energy transfer in a single collision. For thinner layers ($\Omega \lesssim T_m$), the Gaussian approximation becomes insufficient and a more general formalism is applied, which is based upon the Bothe-Landau formula [5–7]. However, in many cases, especially for ions at moderate velocities, significant effects may be due to the charge exchange by electron capture and loss.

The statistical description of energy loss in the presence of charge exchange is considerably more complicated than for pointlike particles. At the very least, one has to account for a significant dependence of the stopping power and, more generally, the differential energy-loss cross section on the instantaneous charge state of the ion. In the presence of charge exchange, one has to deal with a set of cross sections $d\sigma_I(T)$ for every charge state I and a transition is equivalent to abrupt switching from one cross section to another. The energy-loss spectrum is therefore formed by the superposition of collision statistics for a given charge state and statistics of charge-state transitions governed by electron-loss–capture cross sections. It depends on the initial and final charge states of the ion and therefore forms a matrix.

Moreover, charge-changing collisions may represent an important mechanism of the energy loss affecting the spectrum. Accordingly, in general, one has to characterize the energy loss by a whole matrix of cross sections $d\sigma_{IJ}(T)$ depending on the charge state before (I) and after (J) a collision. The minimum energy consumed in a capture-loss cycle is the energy of an electron at the velocity of the ion. Differential cross sections $d\sigma_{IJ}$ for charge-changing collisions ($I \neq J$) differ qualitatively from those for a frozen charge state ($I=J$).

Due to these factors, the statistical description of energy-loss spectra in the presence of charge exchange is associated with considerable mathematical difficulties. Early theoretical estimates [8–11] addressed primarily average energy loss and straggling and were mainly based upon a simplified model neglecting the energy loss in charge-changing collisions and assuming the stopping power to be proportional to the square of the ionic charge. Important progress in the topic had been achieved when the Bothe-Landau formula was generalized to include charge exchange [12,13]. This allowed a powerful and sufficiently general formalism [13,14] that was used to study the low moments of the spectrum, the mean energy loss, the straggling, etc. [13–17], and to calculate the spectra in specific cases [18,17,14]. An efficient technique for direct numerical evaluation of the generalized Bothe-Landau formula was discussed in Ref. [19].

This formula, as it stands, is not convenient for a direct computation of the spectra; it can hardly be handled analytically even for the simplest cases. Furthermore, a direct evaluation requires the complete set of differential cross sections $d\sigma_{IJ}(T)$, which are rarely available for a given system. These circumstances warrant a reduction of the necessary input characterizing elementary events.

Such an approach, valid for relatively large path lengths, is developed in the present paper. The method employed for approximate evaluation of the Bothe-Landau formula is a generalization of a powerful steepest-descent technique outlined in Ref. [20] for pointlike particles. Below, analytical approximations for the energy-loss spectrum and its parameters (the peak energy loss, the half-widths, etc.) are found, which have high accuracy in a wide region of validity ($\Omega \gtrsim T_m$). Being derived *without* specifying explicit cross-sectional input, these approximations are very general and represent readily calculable expressions. General properties of the spectra at large path lengths are primarily determined

*Present address: Physics Department, Odense University, DK-5230 Odense M, Denmark.

by statistical laws rather than by the underlying physics of elementary events.

II. ENERGY-LOSS SPECTRUM AND EIGENVALUE EXPANSION

A. Notation and starting relations

In the presence of charge exchange, the energy-loss spectrum of a particle can be described by the matrix $||F_{IJ}(\Delta E,x)||=\mathbf{F}(\Delta E,x)$, $I,J=1,2,\ldots,n$, where n is the number of available charge states. $F_{IJ}(\Delta E,x)d(\Delta E)$ is the probability for a particle occupying an initial charge state I to occupy state J at path length x and to have lost energy $[\Delta E,d(\Delta E)]$ [13]. The spectrum satisfies the normalization condition

$$\sum_J \int F_{IJ}(\Delta E,x)d(\Delta E)=1 \tag{1}$$

and is determined by the generalized Bothe-Landau formula [12,13]

$$\mathbf{F}(\Delta E,x)=\frac{1}{2\pi}\int_{-\infty}^{\infty} e^{ik\Delta E}e^{Nx\mathbf{Q}(k)}dk, \tag{2}$$

where N is the volume density of atoms (or molecules) of the medium and $\mathbf{Q}(k)$ is a matrix with the elements

$$Q_{IJ}(k)=\int_T e^{-ikT}d\sigma_{IJ}(T)-\delta_{IJ}\sum_L \int_T d\sigma_{IL}(T). \tag{3}$$

Here $d\sigma_{IJ}(T)$ represents the differential cross section for a transition $I\rightarrow J$ accompanied by an energy loss (T,dT).

Formula (2) is valid under the following assumptions [12,13]: uniform random medium, statistical independence of successive collisions, and energy loss sufficiently small to neglect variations in cross sections over the path length x. A derivation of formula (2) is sketched in Appendix A. For pointlike particles $(n=1)$, $\mathbf{Q}(k)$ in Eq. (2) is reduced to the scalar function

$$Q(k)=-\int_T (1-e^{-ikT})d\sigma(T) \tag{4}$$

and Eq. (2) becomes equivalent to the standard Bothe-Landau formula [5–7,12,20]. In the discussion below, general results will occasionally be illustrated by the relatively simple case of a system with two charge states $(n=2)$.

B. Eigenvalue expansion

Let $q^{(\nu)}(k)$, $\nu=1,\ldots,n$, be the set of (generally complex) eigenvalues of the matrix $\mathbf{Q}(k)$, and $\boldsymbol{\beta}^{(\nu)}(k),\boldsymbol{\tau}^{(\nu)}(k)$ the corresponding eigenvectors of the matrix and its transpose:

$$\mathbf{Q}\boldsymbol{\beta}^{(\nu)}=q^{(\nu)}\boldsymbol{\beta}^{(\nu)}, \quad \mathbf{Q}^T\boldsymbol{\tau}^{(\nu)}=q^{(\nu)}\boldsymbol{\tau}^{(\nu)}. \tag{5}$$

It is convenient to normalize the vectors $\boldsymbol{\beta}^{(\nu)}(k)$ and $\boldsymbol{\tau}^{(\nu)}(k)$ by the condition

$$(\boldsymbol{\beta}^{(\nu)},\boldsymbol{\tau}^{(\mu)})\equiv\sum_{I=1}^{n}\beta_I^{(\nu)}\tau_I^{(\mu)}=\delta_{\nu\mu}. \tag{6}$$

Using the column vectors $\boldsymbol{\beta}^{(\nu)}(k)$ and the row vectors $\boldsymbol{\tau}^{(\nu)}(k)$ to form the matrices $\mathbf{B}(k)$ and $\mathbf{B}^{-1}(k)$, respectively, one represents $\mathbf{Q}=\mathbf{B}\mathbf{q}\mathbf{B}^{-1}$, where $\mathbf{q}$ is the diagonal matrix with elements $q^{(1)},q^{(2)},\ldots$. Then one has for the matrix exponential $\exp[Nx\mathbf{Q}]=\mathbf{B}\ \exp[Nx\mathbf{q}]\mathbf{B}^{-1}$ and formula (2) is rewritten as

$$\mathbf{F}(\Delta E,x)=\frac{1}{2\pi}\int_{-\infty}^{\infty} e^{ik\Delta E}\sum_\nu \mathbf{F}^{(\nu)}(k)e^{Nxq^{(\nu)}(k)}dk, \tag{7}$$

where the matrices $\mathbf{F}^{(\nu)}(k)$ are expressed in terms of the eigenvectors

$$F_{IJ}^{(\nu)}=\beta_I^{(\nu)}\tau_J^{(\nu)}. \tag{8}$$

The representation (7),(8) can be used for a direct numerical tabulation of the energy-loss spectrum for a given set of cross sections [19]: Eigenvalues and eigenvectors of the matrix $\mathbf{Q}(k)$ are tabulated for a grid of k values with the forthcoming numerical evaluation of the integral (7). In general, eigenvalues $q^{(\nu)}$ may be determined by solving numerically the characteristic equation $\det||Q_{IJ}-q\delta_{IJ}||=0$; for a small number of charge states $(n\leqslant 4)$, analytical solutions are available. It is convenient to define $q^{(\nu)}(k)$ as continuous functions and the function vanishing at $k=0$ will be denoted as $q^{(1)}(k)$: $q^{(1)}(0)=0$. For a two-state system $(n=2)$, denoting $\mathrm{Sp}\mathbf{Q}=Q_{11}+Q_{22}$, $D=(Q_{11}-Q_{22})^2+4Q_{12}Q_{21}$, and interpreting $\sqrt{D}$ as the value of the square root with a positive real part, one has

$$q^{(1)}(k)=\frac{1}{2}[\mathrm{Sp}\mathbf{Q}(k)+\sqrt{D(k)}],$$

$$q^{(2)}(k)=\frac{1}{2}[\mathrm{Sp}\mathbf{Q}(k)-\sqrt{D(k)}] \tag{9}$$

for small values of k; the signs at $\sqrt{D}$ alterate if and when $D(k)$ comes through a real negative value.

C. Charge-state equilibrium

Integration of $F_{IJ}(\Delta E,x)$ over ΔE yields[1] the charge-state distribution $F_{IJ}(x)$ [13]:

$$\mathbf{F}(x)=e^{Nx\mathbf{Q}(0)}=\sum_\nu \mathbf{F}^{(\nu)}(0)e^{Nxq^{(\nu)}(0)}, \tag{10}$$

where

[1]This and similar derivations are most easily performed via the representation $e^{Nx\mathbf{Q}(k)}=\int_{-\infty}^{\infty}e^{-ik\Delta E}\mathbf{F}(\Delta E,x)d(\Delta E)$ [cf. Eq. (2) and Appendix A], which, in particular, gives Eq. (10) for $k=0$. Note that integration here may be performed with the limits $\pm\infty$, regardless of the possible existence of lower or upper boundaries of ΔE: Formula (2) will automatically produce $\mathbf{F}(\Delta E,x)=0$ outside such boundaries (for example, for $\Delta E<0$).

$$\mathbf{Q}(0)\equiv\mathbf{Q}(k=0)=\sum_L (\delta_{LJ}-\delta_{IJ})\sigma_{IL}, \tag{11}$$

$\sigma_{IL}\equiv\int_T d\sigma_{IL}(T)$ being the total cross sections of state transitions. The properties of the eigenvalues at $k=0$ were considered in Ref. [13]. It can be easily checked that $\Sigma_J Q_{IJ}(0)=0$; hence $\boldsymbol{\beta}^{(1)}(0)=\{1,1,\ldots,1\}$ is an eigenvector of $\mathbf{Q}(0)$ corresponding to the eigenvalue $q^{(1)}(0)=0$. All other eigenvalues have negative real parts (this is a special case of a more general theorem considered in Appendix C):

$$q^{(1)}(0)=0; \quad \mathrm{Re}\ q^{(\nu)}<0, \ \nu\neq 1. \tag{12}$$

In particular, $q^{(\nu)}(0)$ are real in the two-state case: $q^{(1)}(0)=0$, $q^{(2)}(0)=-(\sigma_{12}+\sigma_{21})$; cf. Eq. (9). The eigenvector $\boldsymbol{\tau}^{(1)}(0)$ has real non-negative components and determines the equilibrium charge-state distribution

$$F_{IJ}(x)\simeq F_{IJ}^{(1)}(0)=\tau_J^{(1)}(0)$$

for large x when

$$e^{Nx\mathrm{Re}\ q^{(\nu)}(0)}\ll 1, \quad \nu\neq 1. \tag{13}$$

The associated term in the expansion (7) determines the spectrum for sufficiently large x:

$$\mathbf{F}(\Delta E,x)\simeq\frac{1}{2\pi}\int_{-\infty}^{\infty}\mathbf{F}(k)e^{ik\Delta E+Nxq(k)}dk, \tag{14}$$

where $q(k)\equiv q^{(1)}(k)$ and $\mathbf{F}(k)\equiv\mathbf{F}^{(1)}(k)$. A general theorem to this effect, valid for all physically relevant cross sections, is proved in Appendix B. It turns out in particular that the relative contributions of the $\nu\neq 1$ terms in expansion (7) to the main part of the spectrum are exponentially small for sufficiently large x.

The asymptotic expression (14) significantly simplifies the analysis of energy-loss spectra for large path lengths. It will be shown in Sec. III and Appendix C that the analytical properties of $q(k)$ are in many respects similar to those of $Q(k)$ for pointlike particles [Eq. (4)]. Therefore, analytical methods initially developed for the one-state case may be successfully applied to Eq. (14) with only minor modifications.

It is assumed below that x is large enough for Eq. (14) to be valid. However, caution is indicated: A universal simple criterion for how large the path length should be has not been found. For many important cases, the limitations on the appropriate path lengths can be shown to be synonymous with the charge-state equilibrium condition (13). Several such examples are briefly considered in Appendix B.

III. APPROXIMATE EXPRESSIONS FOR THE SPECTRUM

A. Steepest-descent integration [6,20]

For sufficiently large x, the integral (14) receives its main contribution from the vicinity of a point k_0 in the complex plane where the exponent is stationary:

$$\Delta E=iNx\left.\frac{\partial q(k)}{\partial k}\right|_{k=k_0}\equiv iNxq'(k_0). \tag{15}$$

This implies the proper choice of the path of integration, namely, it should come through the saddle point $k=k_0$ as the line of steepest descent [21].

For pointlike particles, the saddle point $k_0(\Delta E)$ is known to be located at the imaginary axis of k [20]. For an arbitrary number of charge states, the analytical properties of eigenvalues along the imaginary axis are considered in Appendix C. It is shown in particular that the saddle point is also located at the imaginary axis for any value of ΔE: $k_0(\Delta E)=ik_0'(\Delta E)$ with real k_0'; in addition, $F_{IJ}(ik_0')$ is real nonnegative, $q'(ik_0')$ imaginary, and $q''(ik_0')$ real negative.

As shown in Appendix C, the function $q(k)$ at the imaginary axis may be determined algebraically as the (real) eigenvalue of the matrix $\mathbf{Q}(ik')$, which is larger than the real parts of all others. In the two-state case, one may use formula (9) for the eigenvalues at any $k=ik'$ as $D(k)$ is real positive along the imaginary axis.

Letting the path of integration go through k_0 parallel to the real axis, one has for sufficiently large x

$$\mathbf{F}(\Delta E,x)\simeq\frac{1}{2\pi}\int_{-\infty}^{\infty}\{\mathbf{F}(ik_0')[1+Nx\tilde{k}^3q'''(ik_0')/6] + \tilde{k}\mathbf{F}'(ik_0')\}e^{-k_0'\Delta E+Nx[q(ik_0')+\tilde{k}^2q''(ik_0')/2]}d\tilde{k}$$

and integration results in the asymptotic expression

$$\mathbf{F}(\Delta E,x)\simeq\frac{\mathbf{F}(k_0)}{[-2\pi Nxq''(k_0)]^{1/2}}e^{ik_0\Delta E+Nxq(k_0)}. \tag{16}$$

It is not generally possible to analytically extract k_0' as a function of ΔE from Eq. (15). However, one may express ΔE and $\mathbf{F}$ as functions of an auxiliary variable k_0' [20]:

$$\Delta E=iNxq'(ik_0'), \tag{17a}$$

$$\mathbf{F}(\Delta E,x)\simeq\frac{\mathbf{F}(ik_0')}{[-2\pi Nxq''(ik_0')]^{1/2}}e^{-Nx[ik_0'q'(ik_0')-q(ik_0')]}. \tag{17b}$$

Equations (17) allow one to tabulate $F_{IJ}(\Delta E,x)$ versus ΔE for a given x provided that $q(ik')$ and $F_{IJ}(ik')=\beta_I(ik')\tau_J(ik')$ have been found. The range of validity of Eq. (17) and its accuracy will be discussed in Sec. III C.

B. Simple approximations

In this section limiting cases are considered that lead to simple analytical expressions for sufficiently large path lengths. In the limit of large x, the exponential in Eq. (17) becomes small once $Nx|q''(0)|k_0'^2/2\gg 1$. Therefore, apart from exponentially small tails, the spectrum is determined by Eqs. (17) with small values of $k_0'\lesssim 1/\sqrt{Nx|q''(0)|}$. Then, expanding Eq. (17a) in powers of k_0', one can extract explicitly k_0' versus ΔE.

The first approximation

$$k_0'\simeq-\frac{\Delta E-iNxq'(0)}{Nxq''(0)}$$

yields a Gaussian asymptote

$$\mathbf{F}(\Delta E,x)\simeq\frac{1}{\sqrt{2\pi\Omega^2}}\mathbf{F}(0)e^{-\epsilon^2/2}, \tag{18}$$

where $\epsilon=[\Delta E-iNxq'(0)]/\Omega$ and $\Omega^2=-Nxq''(0)$. This property is similar to the well-known one-state case [1].

However, the Gaussian approximation is too rough for many cases of practical interest since the relative error of Eq. (18) in the main part of the spectrum may be $\sim T_m/\Omega$. Significantly better accuracy is provided by taking the next term in k_0' into account:

$$k_0'\simeq\frac{\epsilon}{\Omega}\left[1+\frac{iNxq'''(0)\epsilon}{2\Omega^3}\right].$$

This yields a three-term diffusion approximation

$$\mathbf{F}(\Delta E,x)\simeq\left\{\mathbf{F}(0)\left[1+\frac{iNxq'''(0)}{6\Omega^3}(3\epsilon-\epsilon^3)\right]+\frac{i\mathbf{F}'(0)}{\Omega}\epsilon\right\}\frac{e^{-\epsilon^2/2}}{\sqrt{2\pi\Omega^2}}, \tag{19}$$

which was derived in Ref. [19] directly from Eq. (7). Expressions for the coefficients in formulas (18) and (19) are given in Appendix D.

C. Regions of validity

For pointlike particles, energy-loss spectra for a set of model cross sections, where the Bothe-Landau integral can be evaluated analytically, were compared with the steepest-descent approximation in Ref. [20]. Although in some specific cases formula (17) may even represent the *exact* spectrum [20], terms of relative order $\sim(Nx)^{-1}$ have been neglected in the derivation of Eq. (17). More terms can be taken into account if necessary; an analysis of these terms shows that half-widths and the most probable energy loss are predicted by the one-term approximation (17) with even better accuracy [relative error $\sim(Nx)^{-2}$] than that of the spectrum itself [20].

Therefore, one may expect formula (17) to give a reasonable approximation for the energy-loss spectrum down to path lengths corresponding to $\Omega\sim T_m$. An illustrative practical example will be considered below.

For sufficiently large x the three-term diffusion approximation (19) provides a numerical accuracy comparable to Eq. (17), it represents a simple analytic expression, and it is readily calculable when only the three first moments of the collision cross sections are known [19]. However, while Eq. (17) determines an approximation for the whole spectrum for large x, the three-term diffusion approximation is valid only for ΔE not too far from the maximum. Thus, for any x, the tails of the spectrum will not be correctly determined.

D. Example: 32-MeV ^{3}He in carbon

As an illustration for the concepts discussed above, consider energy-loss spectra of 32-MeV ^{3}He ions in carbon. In Ref. [23] a number of parameters for this system (charge-exchange cross sections, frozen-charge-state stopping powers, and the average energy consumed in a capture-loss cycle) were extracted from energy-loss spectra measured for path lengths far below charge-state equilibrium. In Ref. [19] the measured parameters were used to compose model cross sections and to evaluate the same spectra numerically from Eq. (7); good agreement with experimental spectra was found, apart from the latter being considerably wider for thin foils due to the finite energy resolution of the experiment.

The path lengths considered here are larger than in [23]. Approximations (17–19) are tested below against spectra obtained by direct numerical evaluation of Eq. (7). The same model cross sections are used as in Ref. [19].

For the chosen parameters, the case $\Omega=T_m$ corresponds to a path length slightly smaller than $x=2000\ \mu\mathrm{g/cm}^2$ and condition (13) of charge-state equilibrium is satisfied for path lengths $x\gtrsim100\ \mu\mathrm{g/cm}^2$. The fraction of neutral atoms is negligibly small, so one has a system with two essential charge states; indices 1 and 2 below refer to He^{1+} and He^{2+}, respectively.

For the relatively large path lengths to be considered, the spectra slightly depend on the initial charge state of the ion: $F_{11}\simeq F_{21}$, $F_{22}\simeq F_{12}$. Therefore, only results for F_{11} and F_{22} are shown below.

It is worth mentioning that, due to the small cross section for electron capture, the spectrum F_{22} is only weakly affected by charge exchange. Thus the set of results for F_{22} illustrates also the applicability of the approximations for the one-state case.

In Figs. 1, 2, and 3, corresponding to $\Omega^2\simeq T_m^2$, $\Omega^2\simeq T_m^2/2$, and $\Omega^2\simeq T_m^2/4$, respectively, the approximations are compared with numerical results. Figure 1 shows that already for $\Omega\simeq T_m$ the steepest-descent and three-term diffusion approximations deliver a good accuracy for the spectrum; except for a narrow region around the maximum, these curves can hardly be distinguished from the exact one. As expected, the accuracy of all approximations decreases for smaller path lengths (Figs. 2 and 3). This is accompanied, for the three-term diffusion approximation, by visible negative values on one of the tails. However, the steepest-descent approximation provides a reasonable accuracy even for these path lengths, apart from the altitude of the maximum for the F_{11} spectrum.

Exact and steepest-descent curves for $\Omega^2\simeq T_m^2/6$ are compared in Fig. 4. For so small path lengths they are characterized by noticeable deviations, especially for the F_{11} spectrum. However, the steepest-descent approximation still gives good estimates for the most probable energy loss and the half-widths of the spectrum.

The Gaussian (18) converges only very slowly to the exact curve with increasing path length [relative error in the main part of the spectrum decreases $\sim(Nx)^{-1/2}$]. Figure 5 compares the Gaussian and exact curves for a significantly larger path length ($\Omega^2\simeq5T_m^2$).

Approximations (17–19) have also been tested against exact curves for several qualitatively different model cross sections, which do not correspond to any particular physical system. In all cases, results were similar to those above: a good accuracy of the steepest-descent and three-term diffusion approximations for $\Omega\gtrsim T_m$ and much worse accuracy and a smaller region of validity of the Gaussian.

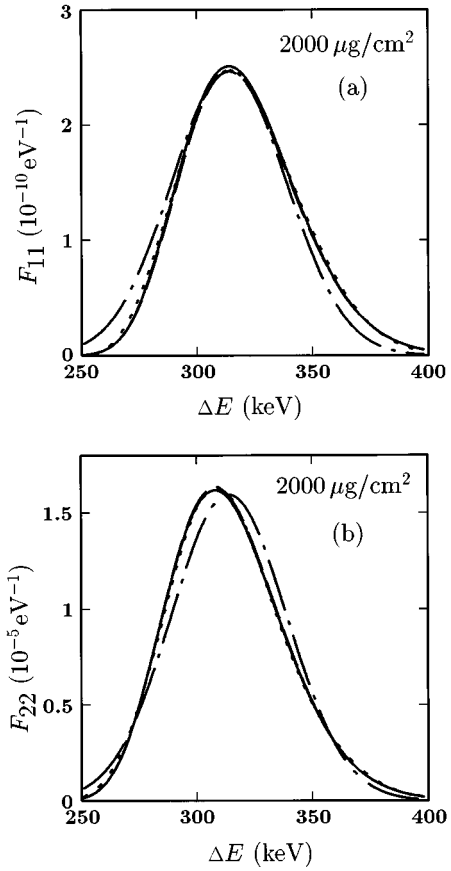

FIG. 1. Comparison of approximations for the energy-loss spectra of 32-MeV ^{3}He ions for path length $x=2000$ μg/cm^2 corresponding to $\Omega \simeq T_m$, for (a) F_{11} and (b) F_{22}. Solid lines, straight numerical evaluation of Eq. (2); dashed lines, steepest-descent approximation (17); dotted lines, three-term diffusion approximation (19); dot-dashed lines, Gaussian (18). Initial and final charge states (a) $I,J=1$ and (b) $I,J=2$.

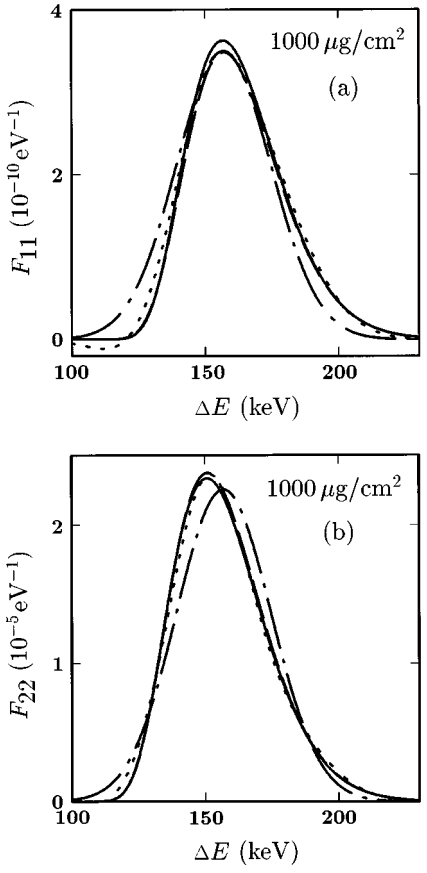

FIG. 2. Same as Fig. 1, but for path length $x=1000$ μg/cm^2 ($\Omega^2 \simeq T_m^2/2$).

IV. PARAMETERS OF THE SPECTRUM

A. Moments

The moments of the energy-loss spectrum in the charge-state equilibrium [13] are easily evaluated from Eq. (14):

$$\langle \Delta E^r \rangle_{IJ} \equiv \frac{\int_0^\infty (\Delta E)^r F_{IJ}(\Delta E,x)\,d(\Delta E)}{\int_0^\infty F_{IJ}(\Delta E,x)\,d(\Delta E)} = \frac{i^r}{F_{IJ}(0)}\frac{\partial^r}{\partial k^r}[F_{IJ}(k)e^{Nxq(k)}]\Big|_{k=0}. \quad (20)$$

In particular, the average energy loss and the straggling can be written as

$$\langle \Delta E \rangle_{IJ} = iNxq'(0) + \frac{iF'_{IJ}(0)}{F_{IJ}(0)}, \quad (21)$$

$$\langle (\Delta E - \langle \Delta E \rangle)^2 \rangle_{IJ} = -Nxq''(0) - \frac{F''_{IJ}(0)}{F_{IJ}(0)} + \left[\frac{F'_{IJ}(0)}{F_{IJ}(0)}\right]^2. \quad (22)$$

Expressions for the coefficients $q'(0), F'_{IJ}(0)$, etc., are given in Appendix D.

B. Peak energy loss

1. General formula

Approximate expressions for the peak (most probable) energy losses $(\Delta E)_{p,IJ}$ can be found similarly to the one-state case [20]. Differentiating $\ln F_{IJ}$ in the Eq. (17b) with respect to $k_0 = ik'_0$, one obtains the equation

$$Nx = \frac{1}{k_{p,IJ}q''(k_{p,IJ})}\left[\frac{F'_{IJ}(k_{p,IJ})}{F_{IJ}(k_{p,IJ})} - \frac{q'''(k_{p,IJ})}{2q''(k_{p,IJ})}\right] \quad (23)$$

for the value $k_{p,IJ}$ of the running variable k_0 corresponding to the maximum of the distribution $F_{IJ}(\Delta E,x)$. Once $k_{p,IJ}$ has been found, the peak energy loss is determined by Eq. (17a):

$$(\Delta E)_{p,IJ} = iNxq'(k_{p,IJ}). \quad (24)$$

Equation (23) shows that $k_{p,IJ}$ is small for large x. Expansion in powers of $k_{p,IJ}$ gives

$$k_{p,IJ} = \frac{1}{Nxq''(0)}\left[\frac{F'_{IJ}(0)}{F_{IJ}(0)} - \frac{q'''(0)}{2q''(0)}\right] + O\left(\frac{1}{(Nx)^2}\right) \quad (25)$$

and, from Eq. (24),

$$(\Delta E)_{p,IJ} = iNxq'(0) + i\left[\frac{F'_{IJ}(0)}{F_{IJ}(0)} - \frac{q'''(0)}{2q''(0)}\right] + O\left(\frac{1}{Nx}\right). \quad (26)$$

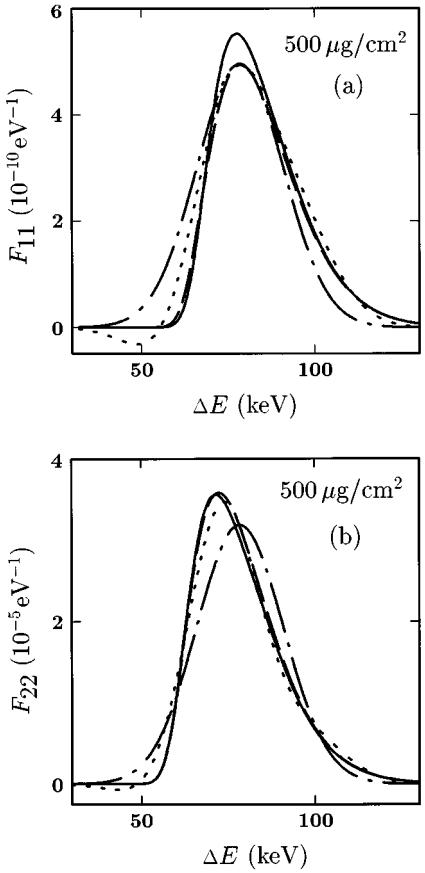

FIG. 3. Same as Fig. 1, but for path length $x=500\ \mu g/cm^2$ ($\Omega^2 \simeq T_m^2/4$).

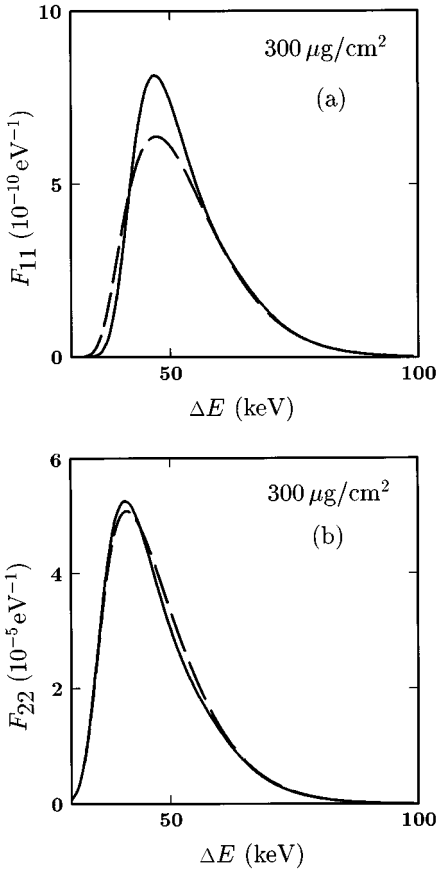

FIG. 4. Energy-loss spectra of 32-MeV ^{3}He ions in carbon for path length $x=300\ \mu g/cm^2$ ($\Omega^2 \simeq T_m^2/6$). Solid lines, straight numerical evalution of Eq. (2); dashed lines, steepest-descent approximation (17). Initial and final charge states (a) $I,J=1$ and (b) $I,J=2$.

This formula determines the leading terms of the asymptotic expansion for the peak energy loss. Compare Eq. (26) with the average energy loss

$$\langle \Delta E \rangle_{IJ} - (\Delta E)_{p,IJ} = i \frac{q'''(0)}{2q''(0)} + O\left(\frac{1}{Nx}\right). \qquad (27)$$

Like in the one-state case [20], the leading asymptotic term in this difference does not depend on x. Also, it does not depend on the initial (I) or final (J) charge state.

For pointlike particles, formula (27) is reduced to a well-known expression [20]

$$\langle \Delta E \rangle - (\Delta E)_p = \frac{\int T^3 d\sigma(T)}{2\int T^2 d\sigma(T)} + O\left(\frac{1}{Nx}\right). \qquad (28)$$

In the presence of charge exchange, explicit expressions for the asymptotic difference between the peak and mean energy loss become much more complicated. General formulas for the calculation of the parameters $q''(0)$ and $q'''(0)$ are given in Appendix D. The following qualitative differences between Eqs. (28) and (27) for $n>1$ should be mentioned.

(i) For pointlike particles, the asymptotic value of $\langle \Delta E \rangle - (\Delta E)_p$ depends only on the second and third moments of the collision cross section and therefore is mainly determined by properties of very close collisions of ions with target electrons. In the presence of charge exchange, there may be also a significant dependence on the first moments of the cross sections, i.e., in particular, on the contribution of distant collisions into ion stopping.

(ii) In accordance with formula (28), for large path lengths $\langle \Delta E \rangle$ always exceeds $(\Delta E)_p$ in the case of pointlike particles. However, for $n>1$ the asymptotic value of $\langle \Delta E \rangle - (\Delta E)_p$ may well be negative for some parameters.

2. The generalized Landau-Vavilov case

As an illustration, consider a simple model for a two-state case ($n=2$). Apart from its relative simplicity, this model is sensible for a description of the energy-loss spectrum of light high-energy ions. Assume the free Coulomb cross section for close frozen-charge-state collisions [4,5,7,20]

$$d\sigma_{II}(T) \simeq \frac{W_B}{T_m}\frac{dT}{T^2}, \quad T \sim T_m = 2mv^2, I=1,2, \qquad (29)$$

where $W_B = 4\pi Z_1^2 Z_2 e^4$ is Bohr's straggling parameter [4], Z_1 and Z_2 are atomic numbers of the ion and the target, m is the electron mass, and v is the ion velocity. One has then for the moments $\int T^r d\sigma_{II}(T) \simeq W_B T_m^{r-2}/(r-1)$ for $r \geq 2$.

For pointlike particles, assumption (29) corresponds to the well-known Landau-Vavilov case [5,7,20] and the asymptotic mean-to-peak interval is [20]

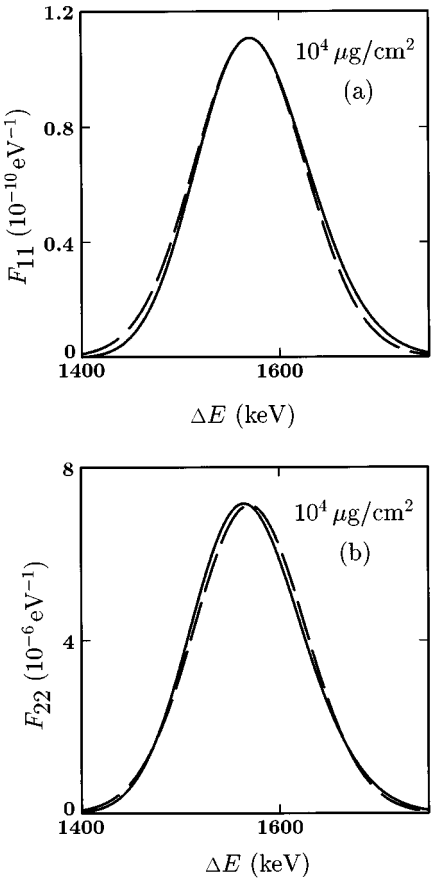

FIG. 5. Illustration of the approach of spectra to the Gaussian form: 32-MeV ^{3}He ions in carbon for path length $x=10^4$ μg/cm^2 ($\Omega^2\simeq 5T_m^2$). Initial and final charge states (a) $I,J=1$ and (b) $I,J=2$. Solid lines, exact curves. The straight numerical evaluation of Eq. (2) and approximations (17) and (19) deliver indistinguishable results. Dashed lines, Gaussian (18).

$$\langle \Delta E\rangle-(\Delta E)_p\simeq\frac{T_m}{4}. \tag{30}$$

Take also the following model cross sections for charge-changing collisions:

$$d\sigma_{12}(T)=\sigma_{12}\delta(T-\varepsilon_1)dT,\quad d\sigma_{21}(T)=\sigma_{21}\delta(T-\varepsilon_2)dT,$$

with a constant $\varepsilon=\varepsilon_1+\varepsilon_2$ representing the average energy consumed in a capture-loss cycle.[2]

Applying the general formulas of Appendix D, one finds a mean-to-peak interval for this model from Eq. (27). Omitting indices I,J on the left-hand side, one has

$$\langle \Delta E\rangle-(\Delta E)_p\simeq\frac{iq'''(0)}{2q''(0)}=\frac{1}{4}\,\frac{T_m+\varepsilon\beta(16+3\eta\xi)}{1+2\beta\eta}, \tag{31}$$

with dimensionless parameters

$$\beta=\bar{\sigma}_{12}\bar{\sigma}_{21}\sigma\varepsilon^2/16W_B,\quad \eta=(P+\bar{\sigma}_{12})^2+(P-\bar{\sigma}_{21})^2,$$

$$\xi=(\bar{\sigma}_{12}-\bar{\sigma}_{21})P-2\bar{\sigma}_{12}\bar{\sigma}_{21},$$

where $\sigma=(\sigma_{12}+\sigma_{21})/2$, $\bar{\sigma}_{IJ}=\sigma_{IJ}/\sigma$, $P=\Delta S/\sigma\varepsilon$, and $\Delta S\equiv\int T[d\sigma_{11}(T)-d\sigma_{22}(T)]$ is the difference between the frozen-charge-state stopping powers.

For

$$\sigma^2\varepsilon\ll|(\sigma_{12}-\sigma_{21})\Delta S| \tag{32}$$

one may neglect energy loss in charge-changing collisions ($\varepsilon=0$, Vollmer's model [8–11]). This reduces Eq. (31) to the expression

$$\langle \Delta E\rangle-(\Delta E)_p\simeq\frac{8\sigma^5W_BT_m+3\sigma_{12}\sigma_{21}(\sigma_{12}-\sigma_{21})(\Delta S)^3}{8\sigma^2[4\sigma^3W_B+\sigma_{12}\sigma_{21}(\Delta S)^2]}. \tag{33}$$

In particular, this formula predicts $(\Delta E)_p>\langle\Delta E\rangle$ for

$$(\sigma_{12}-\sigma_{21})(\Delta S)^3<-\frac{8\sigma^5W_BT_m}{3\sigma_{12}\sigma_{21}}.$$

To illustrate this property, compose a model system exhibiting both positive and negative values of $\langle\Delta E\rangle-(\Delta E)_p$, depending on the ratio of electron-capture and -loss rates. Take $\varepsilon=0$ and arbitrary values of W_B and T_m. For cross sections (29), the frozen-charge-state stopping powers may be represented in the form

$$S_{II}\equiv\int Td\sigma_{II}(T)=\frac{W_B}{T_m}L_I,$$

with typical values of the logarithmic factors $L_I\sim 10$. Let $L_2>L_1$ (state 2 corresponds to a larger ion charge; σ_{12} and σ_{21} are cross sections for electron loss and capture, respectively). Then, for sufficiently small $\sigma_{12}+\sigma_{21}$ formula (33) predicts $(\Delta E)_p>\langle\Delta E\rangle$ for $\sigma_{21}<\sigma_{12}$ and not too small σ_{21} and $\sigma_{12}-\sigma_{21}$. For large x, having chosen appropriate values of L_I,σ_{IJ}, one easily can draw spectra with $(\Delta E)_p>\langle\Delta E\rangle$ by making use of the three-term diffusion approximation (19). However, this procedure would not deliver a confirmation of the $(\Delta E)_p>\langle\Delta E\rangle$ effect independent from Eqs. (27) and (33) because the factor $iq'''(0)/2q''(0)$ explicitly enters also Eq. (19). So here the effect will be checked directly by numerical evaluation of the generalized Bothe-Landau formula (2) [19]. Let charge states 1 and 2 correspond to the ion charges $(Z_1-1)|e|$ and $Z_1|e|$, respectively. Take the model cross sections

[2]The distinction between energy consumed in electron-loss and -capture collisions is actually of no importance here since only $\varepsilon=\varepsilon_1+\varepsilon_2$ enters asymptotic expression for the mean-to-peak interval. Indeed, in accordance with Eq. (27), the asymptotic mean-to-peak interval is common for all spectra F_{IJ}, while spectra F_{11} and F_{22} are made up of particles that have suffered an equal number of electron-loss and -capture collisions and therefore may not depend on ε_1 and ε_2 separately.

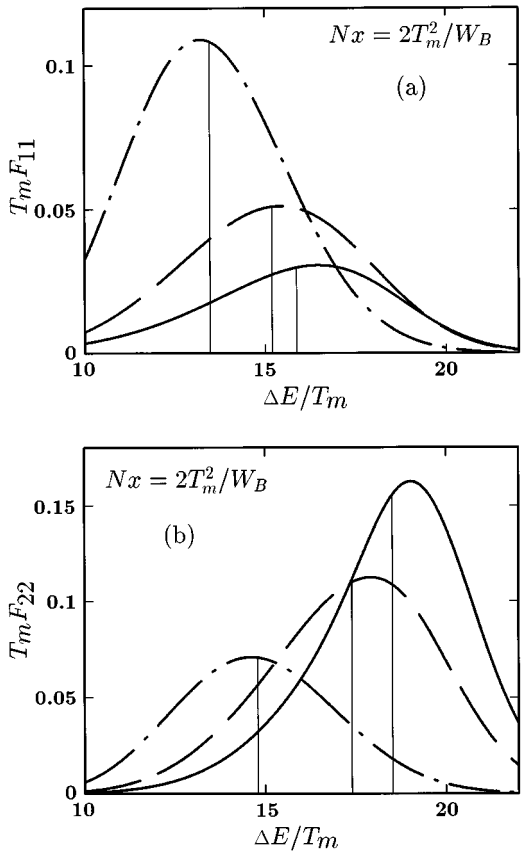

FIG. 6. Illustration of the change of sign of $\langle \Delta E \rangle - (\Delta E)_p$: energy-loss spectra (a) F_{11} and (b) F_{22} for model cross sections (34) and $Nx = 2T_m^2/W_B$. Vertical solid lines show values of the mean energy loss for every spectrum. The model parameters are $Z_1 = 2$, $2L_1 = L_2 = 10$, and $\sigma_{12} = 3W_B/T_m^2$; W_B and T_m are arbitrary. Solid, dashed, and dot-dashed lines correspond to $\sigma_{21}/\sigma_{12} = 1/4$, 1/2, and 3/2, respectively. The corresponding values of $\langle \Delta E \rangle - (\Delta E)_p$ predicted by the asymptotic formula (33) are $-0.74T_m$, $-0.32T_m$, and $0.22T_m$.

$$d\sigma_{II}(T) = \frac{W_B}{T_m}\frac{dT}{T^2} \times \begin{cases} 1 & \text{for } I=2 \text{ or } I=1,\ T_t \leqslant T \leqslant T_m \\ (Z_1-1)^2/Z_1^2 & \text{for } I=1,\ T_{\min} \leqslant T < T_t, \end{cases} \tag{34}$$

where the parameters $T_{\min}$ and T_t are determined from the conditions:

$$\ln\frac{T_m}{T_{\min}} = L_2, \quad \ln\frac{T_m}{T_t} + \frac{(Z_1-1)^2}{Z_1^2}\ln\frac{T_t}{T_{\min}} = L_1.$$

Numerically evaluated spectra F_{11} and F_{22} are shown in Figs. 6(a), and 6(b), respectively, for $Z_1 = 2$, $2L_1 = L_2 = 10$, and $\sigma_{12} = 3W_B/T_m^2$. The spectra are shown for three values of σ_{21} and, in accordance with the above consideration, exhibit $(\Delta E)_p > \langle \Delta E \rangle$ for $\sigma_{12} > \sigma_{21}$ and vice versa. To make the difference between the mean and peak energy loss clearly visible, the spectra are given here for a relatively small path length; this accounts for discrepancies between $\langle \Delta E \rangle - (\Delta E)_p$ for F_{11} and F_{22} and $\sim 50\%$ deviations from the values predicted by formula (33). These discrepancies quickly disappear with further increasing path length.

Note the specific form of condition (32). Even for small energy loss in charge-changing collisions ($\sigma\varepsilon \ll \Delta S$), Vollmer's model may lead to qualitatively incorrect prediction of the mean-to-peak interval if cross sections for electron capture and loss are close to each other. For example, for $\sigma_{12} = \sigma_{21} \equiv \sigma$ one has from Eq. (31):

$$\langle \Delta E \rangle - (\Delta E)_p \simeq \frac{4\sigma W_B T_m + \sigma^2\varepsilon^3 - 3\varepsilon(\Delta S)^2}{4[4\sigma W_B + \sigma^2\varepsilon^2 + (\Delta S)^2]}. \tag{35}$$

Setting $\varepsilon = 0$ here, one has

$$\langle \Delta E \rangle - (\Delta E)_p \simeq \frac{\sigma W_B T_m}{4\sigma W_B + (\Delta S)^2},$$

i.e., $\langle \Delta E \rangle > (\Delta E)_p$ for any parameters, while Eq. (35) gives the inverse inequality for $3\varepsilon(\Delta S)^2 > 4\sigma W_B T_m + \sigma^2\varepsilon^3$.

Mention here also another case of practical importance where Vollmer's model is not applicable. For light MeV ions, the cross section for electron capture (say, σ_{21}) may be smaller than that for electron loss by several orders of magnitude. Correspondingly, while $\sigma_{21}\varepsilon \ll |\Delta S|$, $\sigma_{12}\varepsilon$ may be comparable to or larger than ΔS. In particular, for $\sigma_{21}\varepsilon \ll \Delta S \ll \sigma_{12}\varepsilon$ (this corresponds, for example, to the case of 32-MeV He ions in carbon considered in Sec. III D) formula (31) is reduced to

$$\langle \Delta E \rangle - (\Delta E)_p \simeq \frac{W_B T_m + 2\sigma_{21}\varepsilon^3}{4[W_B + \sigma_{21}\varepsilon^2]}, \tag{36}$$

which is always positive and coincides with the one-state-case result (30) for $W_B \gg \sigma_{21}\varepsilon^2$.

Consider briefly the limit transition to the one-state-case in general terms. As it should be, formulas (31), (33), and (35) for the mean-to-peak interval are reduced the one-state-case result (30) if (i) charge states are equivalent to each other with respect to energy loss ($\Delta S \to 0$) and ions do not lose energy in charge-changing collisions ($\varepsilon \to 0$) or (ii) one of the charge states dominates over the other in equilibrium ($\sigma_{12}/\sigma_{21} \to 0$ or $\sigma_{21}/\sigma_{12} \to 0$). However, due to the still implied condition (13), formulas (31), (33), and (35) generally are not reduced to Eq. (30) if *both* σ_{12} and σ_{21} are small. In particular, in the limiting case $\sigma_{IJ} \to 0$ with $\sigma_{12}/\sigma_{21} = \text{const} \neq 0$, one has from Eq. (31):

$$\langle \Delta E \rangle - (\Delta E)_p \simeq \begin{cases} 3(\sigma_{12}-\sigma_{21})\Delta S/(8\sigma^2) & \text{for } \sigma_{12} \neq \sigma_{21} \\ -3\varepsilon/4 & \text{for } \sigma_{12} = \sigma_{21}. \end{cases}$$

Thus a relative smallness of cross sections for electron capture and loss does not mean that the difference between the mean and peak energy loss is close to its one-state value (30). On the contrary, it is for *sufficiently small* values of σ that $\langle \Delta E \rangle - (\Delta E)_p$ may become negative in the formulas above.

C. Half-widths

Expanding Eq. (17a) for small k_0, one has

$$\frac{\Delta E - iNxq''(0)}{iNxq''(0)} = k_0\left(1 + \frac{q'''(0)}{2q''(0)}k_0 + \cdots\right),$$

or, inserting Eqs. (25), and (26),

$$k_0 - k_{p,IJ} = \frac{\delta E_{IJ}}{iNxq''(0)}\left[1 - \frac{q'''(0)}{2q''(0)}\frac{\delta E_{IJ}}{iNxq''(0)} + \cdots\right], \tag{37}$$

where $\delta E_{IJ} = \Delta E - (\Delta E)_{p,IJ}$. Now, expansion of the exponent in Eq. (17b) around its maximum gives

$$\ln\frac{F_{IJ}(\Delta E,x)}{F_{IJ}((\Delta E)_{p,IJ},x)} \simeq -\frac{1}{2}(k_0 - k_{p,IJ})^2 Nxq''(k_{p,IJ}) - \frac{1}{3}(k_0 - k_{p,IJ})^3 Nxq'''(k_{p,IJ}).$$

Substitution of Eq. (37) and simplification within the same accuracy lead to the following representation for the spectrum:

$$F_{IJ}(\Delta E,x) \simeq F_{IJ}(\Delta E_{p,IJ},x)\exp\left\{-\frac{(\delta E_{IJ})^2}{2\Omega^2}\times\left[1 + \frac{iNxq'''(0)}{3\Omega^4}\delta E_{IJ}\right]\right\}, \tag{38}$$

which holds for the main part of the spectrum: for $|\delta E_{IJ}|$ not too large compared with Ω.

The spectrum (38) is skew and the half-widths are given by

$$(\delta E_{IJ})_{\pm 1/2} \simeq \pm\sqrt{2\ln 2}\,\Omega\left[1 \mp \frac{iNxq'''(0)}{6\Omega^3}\sqrt{2\ln 2}\right] \tag{39}$$

and in this accuracy do not depend on either initial or final charge states of the particles. The mean value between the two half-widths is determined as

$$\frac{1}{2}[(\delta E_{IJ})_{+1/2} + (\delta E_{IJ})_{-1/2}] \simeq (\Delta E)_{p,IJ} + \ln 2\frac{iq'''(0)}{3q''(0)} \simeq \langle\Delta E\rangle_{IJ} - \left[\frac{1}{2} - \frac{1}{3}\ln 2\right]\frac{iq'''(0)}{q''(0)}. \tag{40}$$

The quantity $-iNxq'''(0)/2\Omega^2 \equiv iq'''(0)/2q''(0)$ was shown above to determine the mean-to-peak interval for the spectrum and its properties were discussed in detail in Sec. IV B.

V. SUMMARY

The following conclusions are made.

(i) The energy-loss spectrum of charged particles in the presence of charge exchange has been analyzed theoretically under the assumption that collision cross sections do not vary significantly over the trajectory.

(ii) The generalization of the steepest-descent method [20] to include charge exchange delivers an effective and general technique for an approximate evaluation of spectra valid for large path lengths. The derivation of the central formula (17) does not require specification of the number of charge states or collision cross sections.

(iii) The steepest-descent approximation (17) gives a good accuracy for $\Omega \gtrsim T_m$ provided that the ion beam has reached charge-state equilibrium.

(iv) Apart from the tails of the spectrum, a comparable accuracy is provided by the three-term diffusion approximation Eq. (19). Coefficients entering Eq. (19) are determined by the first three moments of the collision cross sections.

(v) The Gaussian approximation is characterized by a poorer accuracy and a smaller region of validity ($\Omega \gg T_m$).

(vi) Energy-loss spectra for 32-MeV ^{3}He ions in carbon have been calculated numerically and compared with results delivered by the approximations.

(vii) The approximations allow one to find asymptotic expansions for the parameters of the spectrum in inverse powers of the path length. Expansions (27) and (39) for the peak energy loss and the half-widths of the spectrum have been derived. The leading terms coincide with the mean energy loss and the standard deviation, respectively. In both expansions, the leading correction terms are independent of the path length as well as initial and final charge states of the particle and are determined by the first three moments of the collision cross sections.

(viii) An asymptotic expression for the mean-to-peak interval has been specified [Eq. (31)] and analyzed for the generalized Landau-Vavilov case. In particular, it has been shown and illustrated on a model system that the asymptotic difference between the peak and mean energy loss may have either sign depending on stopping and charge-exchange parameters.

ACKNOWLEDGMENTS

The author is very grateful to Professor Peter Sigmund for stimulating this work, numerous enlightening discussions, and helpful advice. This work was supported by the Danish Natural Science Research Council (SNF).

APPENDIX A: DERIVATION OF GENERALIZED BOTHE-LANDAU FORMULA

The derivation of formula (2) sketched below is based upon the kinetic equations for the energy-loss spectrum. Originally, this formula was established by another method [12,13].

Let the ion be in a charge state I initially. Over a small path length Δx, it suffers no collisions with the probability $1 - N\Delta x\Sigma_L\int_T d\sigma_{IL}(T)$, while $N\Delta x d\sigma_{IL}(T)$ is the probability of a collision accompanied by an energy loss (T,dT) and a state transition $I \to L$. Accordingly, one identifies the two contributions into the energy-loss spectrum at a larger path length x:

$$F_{IJ}(\Delta E,x)=\left(1-N\Delta x\sum_L \int_T d\sigma_{IL}(T)\right)F_{IJ}(\Delta E,x-\Delta x)$$
$$+N\Delta x\sum_L \int_T d\sigma_{IL}(T)F_{LJ}(\Delta E-T,x-\Delta x)$$
$$+O((\Delta x)^2).$$

For $\Delta x\to 0$, one obtains the backward kinetic equation for $\mathbf{F}(\Delta E,x)$:

$$\frac{\partial F_{IJ}(\Delta E,x)}{\partial x}=N\sum_L \int_T d\sigma_{IL}(T)[F_{LJ}(\Delta E-T,x)$$
$$-F_{IJ}(\Delta E,x)]. \tag{A1}$$

Alternatively, using the balance relation

$$F_{IJ}(\Delta E,x+\Delta x)=\left(1-N\Delta x\sum_L \int_T d\sigma_{JL}(T)\right)F_{IJ}(\Delta E,x)$$
$$+N\Delta x\sum_L \int_T d\sigma_{LJ}(T)F_{IL}(\Delta E-T,x)$$
$$+O((\Delta x)^2),$$

one can establish the forward equation [9]

$$\frac{\partial F_{IJ}(\Delta E,x)}{\partial x}=N\sum_L \int_T [F_{IL}(\Delta E-T,x)d\sigma_{LJ}(T)$$
$$-F_{IJ}(\Delta E,x)d\sigma_{JL}(T)]. \tag{A2}$$

Going over to the Fourier transform

$$\mathbf{F}(k,x)=\int_{-\infty}^{\infty} e^{-ik\Delta E}\mathbf{F}(\Delta E,x)d(\Delta E),$$

one reduces Eqs. (A1) and (A2) to the matrix equations

$$\frac{\partial \mathbf{F}(k,x)}{\partial x}=N\mathbf{Q}(k)\mathbf{F}(k,x),\quad \frac{\partial \mathbf{F}(k,x)}{\partial x}=N\mathbf{F}(k,x)\mathbf{Q}(k), \tag{A3}$$

where the matrix $\mathbf{Q}(k)$ is determined by Eq. (3). Utilizing the boundary condition

$$F_{IJ}(\Delta E,x=0)=\delta_{IJ}\delta(\Delta E),\quad F_{IJ}(k,x=0)=\delta_{IJ},$$

one finds

$$\mathbf{F}(k,x)=e^{Nx\mathbf{Q}(k)} \tag{A4}$$

and backward Fourier transformation delivers formula (2).

APPENDIX B: DOMINANCE OF THE SPECTRUM BY A SINGLE EIGENVALUE FOR LARGE PATH LENGTHS

The purpose of this appendix is to prove that for sufficiently large path lengths the energy-loss spectrum is solely dominated by the $\nu=1$ term in expansion (7); estimates of the pertinent path-length scale will also be given for a few special cases. For simplicity, the explicit discussion below is limited by the case of real k; however, the main results remain valid also if the integration in Eq. (7) is performed along a straight line in the complex plane of k parallel to the real axis.

Since $q^{(1)}(0)=0$, for sufficiently small k the integrand in Eq. (7) is ~ 1 for any x. The relative significance of different contributions in Eq. (7) is primarily governed by the behavior of Re $q^{(\nu)}(k)$: For given values of x and ν, the integral receives exponentially small contributions from those regions of k where Re $q^{(\nu)}(k)<0$ and $Nx|\text{Re } q^{(\nu)}(k)|\gg 1$. Therefore, contributions of all $\nu\neq 1$ terms to the energy-loss spectrum may be neglected if

$$[\text{Re } q^{\nu\neq 1}]_{\max}<0,\quad Nx|[\text{Re } q^{\nu\neq 1}]_{\max}|\gg 1, \tag{B1}$$

where $[\text{Re } q^{\nu\neq 1}]_{\max}$ is the maximum value of Re $q^{(\nu)}(k)$ for all k and $\nu\neq 1$. The first inequality here is crucial for the dominance of the spectrum by a single eigenvalue for large x, while the second specifies the appropriate region of path lengths.

For sufficiently small $|k|$, the functions Re $q^{(\nu)}(k)$ are close to the $k=0$ values $q^{(1)}(0)=0$, Re $q^{(\nu\neq 1)}(0)<0$. For sufficiently large $|k|$, the matrix $\mathbf{Q}(k)$ is dominated by its diagonal elements and all Re $q^{(\nu)}(k)$ have large negative values. Between these two limits, the functions Re $q^{(\nu)}(k)$ can show a variety of different types of behavior for different numbers of charge states and sets of cross sections.

Consider a few specific cases where $[\text{Re } q^{\nu\neq 1}]_{\max}$ can be estimated analytically. A simple case is delivered by those systems where all functions Re $q^{(\nu)}(k)$ decrease monotonically with increasing $|k|$; the example system considered in Sec. III D belongs to this category. In this case, the first condition (B1) is obviously satisfied:

$$[\text{Re } q^{\nu\neq 1}]_{\max}=\max_{\nu\neq 1} q^{(\nu)}(0)<0 \tag{B2}$$

and the second condition (B1) coincides with that of the charge-state equilibrium.

In the case of a triangular matrix $\mathbf{Q}(k)$ (one-way charge exchange), the eigenvalues are equal to diagonal elements of the matrix, Re $q^{(\nu)}(k)<$ Re $q^{(\nu)}(0)$ for any ν and $k\neq 0$, and thus $[\text{Re } q^{\nu\neq 1}]_{\max}$ is again given by Eq. (B2). Consider also a two-state system with a negligible energy loss in charge-changing collisions. For small values of k, the eigenvalues $q^{(\nu)}(k)$ are determined by Eq. (9) with $Q_{IJ}=\sigma_{IJ}$ for $I\neq J$. If the inequalities $d\sigma_{11}(T)\geqslant d\sigma_{22}(T)$, $\sigma_{12}>\sigma_{21}$ (or vice versa) hold; then $D(k)$ never comes through a real negative value, Eq. (9) is valid for any value of k, and therefore $[\text{Re } q^{\nu\neq 1}]_{\max}<-(\sigma_{12}+\sigma_{21})/2$ differs from Eq. (B2) by no more than a factor of 2.

In the general case, finding $[\text{Re } q^{\nu\neq 1}]_{\max}$ may not be possible by analytical means; numerical tabulation is always a feasible option for a particular system. However, the inequality $[\text{Re } q^{\nu\neq 1}]_{\max}<0$ is valid for all physical systems and therefore the spectrum is dominated by $q^{(1)}(k)$ for sufficiently large path lengths. It follows from the following:

Theorem 1. For any physically relevant set of cross sections, all eigenvalues $q^{(\nu)}(k)$ have strictly negative real parts for all real k, the only exception being $q^{(1)}(k=0)=0$.

Proof. Consider the matrix $\mathbf{Q}(k)$ at a real value of k. Diagonal elements of the matrix may be written as

$$Q_{II}(k) = -\sigma_{II}(k) - \sum_{L\,(\neq I)} \sigma_{IL},$$

where $\sigma_{II}(k) = \int_T (1 - e^{-ikT}) d\sigma_{II}(T)$. Let α be a real positive constant such that $\alpha + \mathrm{Re}\ Q_{II}(k) > 0$ for any I. Introduce matrices

$$A_{IJ}(\alpha,k) = \alpha\delta_{IJ} + Q_{IJ}(k),$$

$$B_{IJ}(\alpha,k) = \gamma(\alpha,k)\delta_{IJ} + Q_{IJ}(0),$$

where

$$\gamma(\alpha,k) = \max_I \left\{ \sum_{L\,(\neq I)} \sigma_{IL} + \left[\left(\alpha - \mathrm{Re}\ \sigma_{II}(k) - \sum_{L\,(\neq I)} \sigma_{IL} \right)^2 + [\mathrm{Im}\ \sigma_{II}(k)]^2 \right]^{1/2} \right\}.$$

The complex matrix $\mathbf{A}(\alpha,k)$ has eigenvalues $\alpha + q^{(\nu)}(k)$, $\nu = 1, \ldots, n$. Eigenvalues of the matrix $\mathbf{B}(\alpha,k)$ are given by $\gamma(\alpha,k) + q^{(\nu)}(0)$, $\nu = 1, \ldots, n$, while all its elements are real and non-negative. The easily verified inequality $|A_{IJ}(\alpha,k)| \leq B_{IJ}(\alpha,k)$ and relevant theorems on the properties of the matrices with non-negative elements (see [22], Chap. 13) ensure that the moduli of all eigenvalues of $\mathbf{A}(\alpha,k)$ do not exceed the spectral radius of $\mathbf{B}(\alpha,k)$, i.e.,

$$|q^{(\nu)}(k) + \alpha| \leq \gamma(\alpha,k) + q^{(1)}(0) = \gamma(\alpha,k).$$

Letting $\alpha \to +\infty$, one finds the following upper estimate for Re $q^{(\nu)}$:

$$\mathrm{Re}\ q^{(\nu)}(k) \leq -\min_I \mathrm{Re}\ \sigma_{II}(k) = -\min_I \int_T (1 - \cos kT) d\sigma_{II}(T). \qquad \text{(B3)}$$

At $k = 0$, Re $q^{(\nu)}(0) < 0$ for $\nu \neq 1$; for $k \neq 0$, all functions Re $\sigma_{II}(k)$ are strictly negative (exceptions are possible only in the physically unacceptable cases of either $d\sigma_{II}(T) \equiv 0$ or $d\sigma_{II}(T)$ being a δ function). Therefore, except for $q^{(1)}(k = 0) = 0$, $q^{(\nu)}(k) < 0$ for any k and ν and the proof is completed.

Utilizing results of Appendix C, one can generalize the above argument for the case when integration in formula (7) is performed along a straight line in the complex plane of k parallel to the real axis, like in Sec. III A. Similarly, the dominance of the spectrum by a single eigenvalue for sufficiently large x is guaranteed by the following theorem, valid for all physically relevant sets of cross sections.

Theorem 2. At imaginary $k = ik'$, $q^{(1)}(ik')$ is real and larger than all Re $q^{(\nu)}(ik'), \nu \neq 1$; for any complex k such that Im $k = k'$, Re $k \neq 0$, real parts of all eigenvalues $q^{(\nu)}(k)$ are strictly smaller than $q^{(1)}(ik')$.

APPENDIX C: PROPERTIES OF EIGENVALUES AT THE IMAGINARY AXIS OF k

Let $k = ik'$ with k' real. All elements of the matrix $\mathbf{Q}(ik')$ are real and monotonically increasing functions of k', all nondiagonal elements being non-negative. Therefore, for any finite interval of k' one can choose a positive constant α such that all elements of the matrix $A_{IJ}(k') = \alpha\delta_{IJ} + Q_{IJ}(ik')$ are real, non-negative and monotonically increasing functions of k'. Applying theorems valid for matrices with these properties (see [22], Vol. 2, Chap. 13) and the obvious relations between eigenvalues of matrices A_{IJ} and Q_{IJ}, one proves the following statements.[3]

(i) For any k', the function $q(ik')$ represents a simple real eigenvalue of $\mathbf{Q}(ik')$.

(ii) $q(k)$ is a continuous and monotonically increasing function along the imaginary axis $[dq(ik')/dk' \geq 0]$ and is larger than the real parts of all other eigenvalues $[q(ik') > \mathrm{Re}\ q^{(\nu)}(ik'),\ \nu \neq 1]$.

(iii) For any k', all elements $F_{IJ}(ik')$ are real and non-negative.

(iv) All even-order derivatives of $q(k)$ and $F_{IJ}(k)$ with respect to k are real at the imaginary axis, while all odd-order derivatives are imaginary.

(v) The derivative $dq(ik')/dk'$ has large negative and positive values at $k' \to -\infty$ and $k' \to +\infty$, respectively.

In particular, these statements ensure the existence, for every value of ΔE, of a point $k_0 = k_0(\Delta E) = ik_0'(\Delta E)$ at the imaginary axis satisfying Eq. (15) (i.e., the saddle point) and such that all the quantities $F_{IJ}(ik_0') \geq 0$ and $iq'(ik_0')$, $-q''(ik_0') > 0$ are real.

APPENDIX D: COEFFICIENTS IN APPROXIMATION FORMULAS

The coefficients that enter the approximation formulas for the spectrum (18), (19), and (38) and its basic parameters (Sec. IV) can be calculated in accordance with the following scheme. Differentiate the first relation (5):

$$(\mathbf{Q}' - dq^{(\nu)}/dk)\boldsymbol{\beta}^{(\nu)} = -(\mathbf{Q} - q^{(\nu)}) d\boldsymbol{\beta}^{(\nu)}/dk, \qquad \text{(D1)}$$

where $\mathbf{Q}' \equiv d\mathbf{Q}/dk$. Multiplying this relation by $\boldsymbol{\tau}^{(\nu)}$ and using Eqs. (5) and (6), one finds

$$\frac{dq^{(\nu)}}{dk} = (\mathbf{Q}'\boldsymbol{\beta}^{(\nu)}, \boldsymbol{\tau}^{(\nu)}), \qquad \text{(D2)}$$

where $(\mathbf{Q}'\boldsymbol{\beta}^{(\nu)}, \boldsymbol{\tau}^{(\mu)}) \equiv \Sigma_{I,J} Q_{IJ}' \beta_J^{(\nu)} \tau_I^{(\mu)}$. Now substitute the expansion $d\boldsymbol{\beta}^{(\nu)}/dk = \Sigma_\mu b_{\nu\mu} \boldsymbol{\beta}^{(\mu)}$ with yet unknown coefficients $b_{\nu\mu}$ into Eq. (D1). Multiplying the resulting equation by $\boldsymbol{\tau}^{(\mu)}$ and taking relations (5) and (6) into account, one finds, for $\nu \neq \mu$, $[q^{(\nu)} - q^{(\mu)}] b_{\nu\mu} = (\mathbf{Q}'\boldsymbol{\beta}^{(\nu)}, \boldsymbol{\tau}^{(\mu)})$ and therefore

[3] Strictly, one more requirement should be fulfilled: The matrix A_{IJ} is to be *irreducible* [22], i.e., there should be no disconnected subsets of charge states. If there were, such subsets should be treated separately.

$$\frac{d\boldsymbol{\beta}^{(\nu)}}{dk}=\sum_{\mu\,(\neq\nu)}\frac{1}{q^{(\nu)}-q^{(\mu)}}(\mathbf{Q}'\boldsymbol{\beta}^{(\nu)},\boldsymbol{\tau}^{(\mu)})\boldsymbol{\beta}^{(\mu)}+b_{\nu\nu}\boldsymbol{\beta}^{(\nu)}. \tag{D3}$$

A similar evaluation for $d\boldsymbol{\tau}^{(\nu)}/dk$ gives [coefficient at $\boldsymbol{\tau}^{(\nu)}$ is related to $b_{\nu\nu}$ by condition (6)]

$$\frac{d\boldsymbol{\tau}^{(\nu)}}{dk}=\sum_{\mu\,(\neq\nu)}\frac{1}{q^{(\nu)}-q^{(\mu)}}(\mathbf{Q}'\boldsymbol{\beta}^{(\mu)},\boldsymbol{\tau}^{(\nu)})\boldsymbol{\tau}^{(\mu)}-b_{\nu\nu}\boldsymbol{\tau}^{(\nu)}. \tag{D4}$$

The parameters $b_{\nu\nu}$ are determined by an additional normalization condition and do not enter the final results. Further differentiation of Eq. (D2) and substitution of $\nu=1$, $k=0$, and $q^{(1)}=0$ expresses the required coefficients in terms of eigenvalues and eigenvectors at $k=0$ only:

$$q'(0)=a_{11}^{[1]},\quad q''(0)=a_{11}^{[2]}-\sum_{\mu\,(\neq 1)}\frac{2}{q^{(\mu)}}a_{1\mu}^{[1]}a_{\mu 1}^{[1]},$$

$$q'''(0)=a_{11}^{[3]}-\sum_{\mu\,(\neq 1)}\frac{1}{q^{(\mu)}}\Bigg\{3(a_{1\mu}^{[1]}a_{\mu 1}^{[2]}+a_{1\mu}^{[2]}a_{\mu 1}^{[1]})+\frac{6}{q^{(\mu)}}(a_{11}^{[1]}-a_{\mu\mu}^{[1]})a_{1\mu}^{[1]}a_{\mu 1}^{[1]}-\sum_{\lambda\,(\neq 1,\mu)}\frac{2}{q^{(\lambda)}}[3a_{1\lambda}^{[1]}a_{\lambda\mu}^{[1]}a_{\mu 1}^{[1]}+a_{1\mu}^{[1]}a_{\lambda 1}^{[1]}a_{\mu\lambda}^{[1]}]\Bigg\},$$

$$F_{IJ}'(0)=-\sum_{\mu\,(\neq 1)}\frac{1}{q^{(\mu)}}[a_{1\mu}^{[1]}\beta_I^{(\mu)}\tau_J^{(1)}+a_{\mu 1}^{[1]}\beta_I^{(1)}\tau_J^{(\mu)}],$$

etc., where $q^{(\mu)},\boldsymbol{\beta}^{(\mu)},\boldsymbol{\tau}^{(\mu)}$ are taken at $k=0$,

$$a_{\nu\mu}^{[r]}=(-i)^r(\mathbf{P}^{[r]}\boldsymbol{\beta}^{(\nu)},\boldsymbol{\tau}^{(\mu)})\equiv(-i)^r\sum_{I,J=1}^{n}P_{IJ}^{[r]}\beta_J^{(\nu)}\tau_I^{(\mu)}, \tag{D5}$$

and the matrices $\mathbf{P}^{(r)}$ contain the moments of the cross sections

$$P_{IJ}^{[r]}=\int_T T^r d\sigma_{IJ}(T).$$

In particular, in the two-state case $(n=2)$ $q^{(2)}=-(\sigma_{12}+\sigma_{21})$ and the formulas above are reduced as

$$q'(0)=a_{11}^{[1]},\quad q''(0)=a_{11}^{[2]}+\frac{2}{\sigma_{12}+\sigma_{21}}a_{12}^{[1]}a_{21}^{[1]},$$

$$q'''(0)=a_{11}^{[3]}+\frac{3}{\sigma_{12}+\sigma_{21}}\Bigg[a_{12}^{[1]}a_{21}^{[2]}+a_{12}^{[2]}a_{21}^{[1]}-\frac{2}{\sigma_{12}+\sigma_{21}}(a_{11}^{[1]}-a_{22}^{[1]})a_{12}^{[1]}a_{21}^{[1]}\Bigg],$$

$$F_{IJ}'(0)=\frac{1}{\sigma_{12}+\sigma_{21}}[a_{12}^{[1]}\beta_I^{(2)}\tau_J^{(1)}+a_{21}^{[1]}\beta_I^{(1)}\tau_J^{(2)}],$$

where $a_{IJ}^{[r]}$ are determined by formula (D5) with

$$\boldsymbol{\beta}^{(1)}=\begin{pmatrix}1\\1\end{pmatrix},\quad \boldsymbol{\tau}^{(1)}=\frac{1}{\sigma_{12}+\sigma_{21}}\begin{pmatrix}\sigma_{21}\\\sigma_{12}\end{pmatrix},$$

$$\boldsymbol{\beta}^{(2)}=\frac{1}{\sigma_{12}+\sigma_{21}}\begin{pmatrix}\sigma_{12}\\-\sigma_{21}\end{pmatrix},\quad \boldsymbol{\tau}^{(2)}=\begin{pmatrix}1\\-1\end{pmatrix}.$$

[1] N. Bohr, Mat. Fys. Medd. K. Dan. Vidensk. Selsk. **18**, 8 (1948).
[2] U. Fano, Annu. Rev. Nucl. Sci. **13**, 1 (1963).
[3] M. Inokuti, Rev. Mod. Phys. **43**, 297 (1971).
[4] N. Bohr, Philos. Mag. **30**, 581 (1915).
[5] L. Landau, J. Phys. (Moscow) **8**, 201 (1944).
[6] J. E. Moyal, Philos. Mag. **46**, 263 (1955).
[7] P. V. Vavilov, Zh. Eksp. Teor. Fiz. **32**, 920 (1957) [Sov. Phys. JETP **5**, 749 (1957)].
[8] O. Vollmer, Nucl. Instrum. Methods **121**, 373 (1974).
[9] K. B. Winterbon, Nucl. Instrum. Methods **144**, 311 (1977).
[10] B. Efken, D. Hann, D. Hilscher, and G. Wüstefeld, Nucl. Instrum. Methods **129**, 219 (1975).
[11] C. J. Sofield, N. E. B. Cowern, R. J. Petty, J. M. Freeman, and J. P. Mason, Phys. Rev. A **17**, 859 (1978).
[12] P. Sigmund, in *Interaction of Charged Particles with Solids and Surfaces*, Vol. 271 of *NATO Advanced Study Institute, Series B: Physics*, edited by A. Gras-Marti *et al.* (Plenum, New York, 1991), p. 73.
[13] P. Sigmund, Nucl. Instrum. Methods Phys. Res. B **69**, 113 (1992).
[14] P. Sigmund, Nucl. Instrum. Methods Phys. Res. B **115**, 111 (1996).
[15] P. Sigmund, Phys. Rev. A **50**, 3197 (1994).
[16] A. Närmann and P. Sigmund, Phys. Rev. A **49**, 4709 (1994).
[17] P. Sigmund and N. Närmann, Laser Part. Beams **13**, 281 (1995).
[18] A. Närmann, Phys. Rev. A **51**, 548 (1995).
[19] L. Glazov and P. Sigmund, Nucl. Instrum. Methods Phys. Res. B **125**, 110 (1997).
[20] P. Sigmund and K. B. Winterbon, Nucl. Instrum. Methods Phys. Res. B **12**, 1 (1985).
[21] A. Erdelyi, *Asymptotic Expansions* (Dover, New York, 1956).
[22] F. R. Gantmacher, *The Theory of Matrices* (Chelsea, New York, 1959).
[23] H. Owaga *et al.*, Phys. Rev. B **43**, 11 370 (1991); Phys. Lett. A **160**, 77 (1991); Nucl. Instrum. Methods Phys. Res. B **69**, 108 (1992).